efficiency of gene transduction using this photocured gelatinous matrix was strictly limited because of very low permeation of a giant molecule, *i.e.*, the adenoviral vector, because tissue permeation largely depends on the molecular size of a permeant (18). On the basis of these experimental data, an alternative NK4 delivery system was devised for *in situ* production of NK4 on the diseased tissue. The working principle of the fabricated device under development is that a hybrid tissue, constructed by *ex vivo* gene-transduced autologous cells with a biodegradable mesh, is adhered to a resected tissue. NK4 secreted from the gene-transduced cells in the hybrid tissue is transported deep into the target tissue and suppresses the tumor growth. If this works effectively, such a cell-based delivery system, which is a product of tissue engineering and genetic engineering disciplines, will be a promising therapeutic tool.

In this study, rat OMECs and adenoviral vector-mediated *NK4* gene transduction were used. The fabrication of the tissue-engineered, gene-transduced hybrid tissue, the effects on pancreatic cancer cells *in vitro*, and a xenograft pancreatic cancer model *in vivo* are reported. Its potential applicability in a clinical setting is discussed.

MATERIALS AND METHODS

OMEC. The harvesting and culture of rat OMECs were according to the "feeder layer technique" developed by Rheinwald and Green *et al.* (19–21). Briefly, oral mucosal tissues, which were harvested from 3- to 6-week-old Wistar rats, were cut into small pieces and immersed twice in PBS (pH 7.4; Nissui Pharmaceutical Co., Ltd., Tokyo, Japan) containing antibiotics (1000 units/ml Penicillin G potassium, 1 mg/ml kanamycin, and 2.5 μg/ml amphotericin B) for 30 min at 37°C. Then, these tissues were immersed in DMEM (Life Technologies, Inc., Grand Island, NY) containing 0.2% dispase (Sigma-Aldrich Co., St. Louis, MO) at 4°C for 20 h, followed by treatment with 0.25% trypsin and 5 mM EDTA solution for 30 min at room temperature. The enzyme activity was blocked by washing with DMEM containing 10% FBS (CSL Ltd., Victoria, Australia). Then, the specimens were gently stirred in DMEM containing 5% FBS for 30 min and passed through a 50-μm filter to obtain OMECs.

Swiss 3T3 cells, obtained from Dainippon Pharmaceutical Co., Ltd. (Osaka. Japan) and treated with 4 μg/ml Mitomycin C (Wako Pure Chemical Industries, Tokyo, Japan) for 2 h, were seeded on a six-well plate (Corning Inc., Corning, NY) at a density of 1×10^5/well. OMECs were seeded over them at a density of 1×10^5/well and cultured in 10% CO_2 in epithelium formation medium, which was a 3:1 mixture of DMEM and Ham's F medium (Nihonseiyaku, Tokyo, Japan) and supplemented with 5% FBS, 5 μg/ml insulin (Wako Pure Chemical Industries), 5 μg/ml transferrin (Wako Pure Chemical Industries), 2×10^{-9} M triiodothyronine (Sigma-Aldrich Co.), 10 ng/ml cholera toxin (Sigma-Aldrich Co.), 0.5 μg/ml hydrocortisone (Wako Pure Chemical Industries), 100 units/ml penicillin, 0.1 mg/ml kanamycin, and 0.25 mg/ml amphotericin B. Human recombinant epidermal growth factor (Wako Pure Chemical Industries) was added at 10 ng/ml from 3 days after the inoculation. Seven to 10 days later, the proliferated OMECs became confluent (the yield of cell numbers per rat was 6×10^6 to 1×10^7 cells) and were subcultured. Cells at the second or third passages were used in the present study.

RNA Preparation and RT-PCR. s.c. tissue, which was used as a positive control, was isolated from the back skin of a Wistar rat with scissors under general anesthesia and cut into small pieces. RNA was extracted from OMECs or the pieces of s.c. tissue with ISOGEN-LS (Nippon Gene Co., Ltd., Toyama, Japan) according to the manufacturer's protocol. RNA (35 μg) from each sample was reverse transcribed with a Ready-To-Go T-Primed First-Strand kit (Amersham Pharmacia Biotech, Inc., Piscataway, NJ) according to the manufacturer's protocol. The rat HGF primers used were 5′-AGTAGGGTGGATGGTTAGTT-3′ (sense strand) and 5′-TACAACTTGTATGTCAAAAT-3′ (antisense strand), which delineated a 672-bp product (22). The rat glyceraldehyde-3-phosphate dehydrogenase primer was purchased from R&D Systems, Inc. (Minneapolis, MN). Subsequently, reverse transcription products were PCR amplified, using the rat HGF primer set or the rat glyceraldehyde-3-phosphate dehydrogenase primer set under the following conditions: at 95°C for 5 min followed by 33 cycles at 95°C for 30 s, 60°C for 30 s, and 72°C for 60 s. The amplified products were subjected to electrophoresis in a 1% agarose gel, stained with ethidium bromide, and photographed using a Molecular Imager FX (Bio-Rad Laboratories, Inc., Richmond, CA).

Cell Culture of Cell Lines. Human pancreatic cell lines, AsPC-1 (23) and SUIT-2 (24), generously donated by Dr. H. Iguchi, National Kyushu Cancer Center (Fukuoka, Japan), were cultured in DMEM supplemented with streptomycin, penicillin, and 10% FBS at 37°C in 5% CO_2. The human fibroblast cell line, MRC-5, which secretes biologically active HGF, was obtained from RIKEN Cell Bank (Ibaragi, Japan). The cells were cultured in DMEM supplemented with streptomycin, penicillin, and 10% FBS at 37°C in 5% CO_2.

Preparation of Collagen Membrane and OMEC Sheet. A biodegradable poly(glycolic acid) mesh (knitted-type VICRYL mesh, polyglactin 910; Ethicon, Inc., Somerville, NJ) was placed on a 24-well plate (Greiner Bio-One Co., Ltd., Frickenhausen, Germany), to which a mixture of 0.5 ml of type I collagen (0.3%, CELLGEN; Koken Corp., Tokyo, Japan) and 0.5 ml of DMEM containing 10% FBS was overlayered on the mesh and incubated at 37°C for 30 min to form a collagenous gel-VICRYL mesh hybrid composite. The thick collagenous gel was compressed by a silicone cap to form a dense collagen mesh entrapped in the VICRYL mesh. Cultured OMECs, dislodged with 0.05% trypsin-EDTA, were seeded on the mesh at a density of 2×10^5 cells/cm^2. Two to 3 days later, OMECs formed a subconfluent monolayer. An H&E-stained cross-section of the cell-seeded collagen mesh was observed under a phase-contrast microscope (TE 300; Nikon, Tokyo, Japan). The cell-seeded collagen mesh was fixed in 2% glutaraldehyde (Electron Microscopy Sciences, Washington, PA) for 1 h, then postfixed in 1% osmium tetroxide (Chiyoda Junyaku, Tokyo, Japan) for 1 h, and subsequently dehydrated with a graded series of ethanol, sputter coated with platinum and evaluated by SEM (JEOL, JSM-840A, Tokyo, Japan).

Adenovirus Vectors. The replication-deficient adenovirus vector expressing NK4 (Ad-NK4) used in this study is E1a-, partially E3-deleted vectors based on human adenovirus type 5 (12). Replication-defective E1a, E1b, and E3 recombinant ade-

novirus vector expressing *Escherichia coli* lacZ (Ad-lacZ) was kindly gifted from Professor H. Ueno (University of Occupational and Environmental Health, Fukuoka, Japan; Refs. 25 and 26). The titers of viral stocks were quantified by a plaque-forming assay using 293 cells and expressed as plaque formation unit.

Secretion of NK4 from OMECs *in Vitro*. OMECs, which were plated at 2×10^5 cells/cm^2 on a type I collagen-coated 12-well tissue culture plate (Greiner Bio-One Co., Ltd.) for 72 h, were transduced with Ad-NK4 at an MOI of 10, 50, 100, and 200 in a 500-μl medium at 37°C for 2 h. After transduction, the culture supernatant was replaced with a fresh culture medium. Aliquots of the culture medium were collected every 48 h. The concentration of NK4 in the culture medium was determined using an IMMUNIS human HGF enzyme immunoassay kit (Institute of Immunology, Tokyo, Japan). This ELISA kit has no cross-reactivity between human and rodent HGF.

OMEC Proliferation after Ad-NK4 Transduction *in Vitro*. OMECs, which were seeded at a density of 5×10^4/well on a type I collagen-coated 24-well plate and cultured for 72 h, were transduced with Ad-NK4 or Ad-lacZ at an MOI of 100. Transduced OMECs were cultured in epithelium formation medium. Twenty-four and 48 h later, the cells dislodged using 0.05% trypsin-EDTA were counted using a Coulter counter (Beckman Coulter, Inc., Fullerton, CA).

Invasion Assay. OMECs, which were seeded at a density of 1×10^5 cells/wells on a type I collagen-coated 12-well plate and cultured for 72 h, were transduced with Ad-NK4 or Ad-lacZ at an MOI of 100. After transduction, the culture supernatant was replaced with DMEM containing 2% FBS. Aliquots of the culture medium were collected 3–4 days after transduction (named as NK4-sup and lacZ-sup) and used in invasion assay. The invasion of tumor cells was measured using a 24-well Matrigel invasion double chamber (Becton Dickinson, Bedford, MA). MRC-5 cells were seeded at a density of 1.5×10^4 cells/cm^2 on the outer cup in DMEM containing 10% FBS, and after 24-h cultivation, the medium was replaced by DMEM supplemented with 2% FBS. Pancreatic cancer cells suspended in DMEM containing 2% FBS or NK4-sup were added to the inner cup of Matrigel invasion chamber at a density of 5×10^4 cells/cup. After 24-h cultivation, pancreatic cancer cells that degraded the Matrigel and migrated through 8-μm pores of the membrane at the bottom of the inner cup to the opposite side of the membrane were counted after they were stained with H&E. Five microscopic fields (×200) were randomly selected for cell counting.

Establishment of i.m. Cancerous Mass and Gene Expression. Four-week-old female nude mice (BALB/c nu/nu; Kyudo Co., Ltd., Saga, Japan) were i.m. injected with 3×10^6 AsPC-1 cells in the left flank, and 14 days after injection, Ad-lacZ-transduced OMEC sheets (lacZ-sheets, $n = 9$) or Ad-NK4-transduced OMEC sheets (NK4-sheets, $n = 9$) were implanted s.c. in an upside-down manner as shown in Fig. 1 (27–29). In the control group ($n = 3$), mice were not treated after injection of AsPC-1 cells. Four days after implantation of sheets, tumors with the surrounding tissue were resected. Three samples with lacZ-sheet were embedded in OCT compound for X-gal staining with chromogenic substrate, 5-bromo-4-chloro-3-indolyl-β-galactopyranoside (Sigma-Aldrich Co.), according to the method described previously (30). Ten days after implantation, three samples with lacZ-sheet were also subjected to X-gal staining. The resected tumors of each experimental group ($n = 3$) were washed once in PBS and homogenized with radioimmunoprecipitation assay buffer consisting of 10% 10 × radioimmunoprecipitation assay buffer (Upstate Biotechnology, Inc., Lake Placid, NY), 1 mM sodium orthovanadate (Wako Pure Chemical Industries), and 1 mM phenylmethylsulfonyl fluoride (Wako Pure Chemical Industries), and tumor lysates were obtained. Serum samples were obtained from mice implanted with NK4-sheets ($n = 3$). After protein determinations were performed, the amounts of NK4 in the tumor lysates and sera were analyzed by ELISA, as described above. Seven and 10 days after implantation of NK4 sheets, the amounts of NK4 in the tumor lysates were also examined by ELISA ($n = 3$).

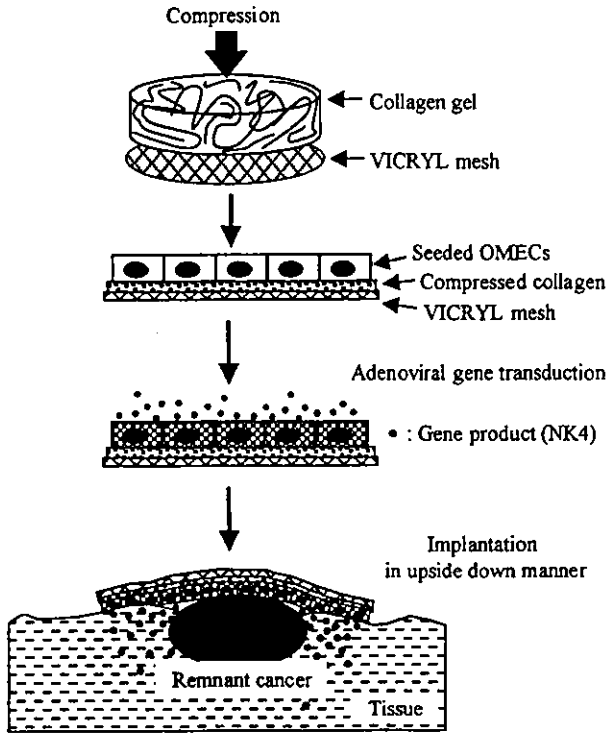

Fig. 1 Schematic of gene-transduced cell sheet and the method of implantation.

Establishment of s.c. Cancerous Mass. To investigate the therapeutic efficacy of the sheet, mice were s.c. injected with 3×10^6 AsPC-1 cells in the left flank on day 0. Three days after s.c. injection, lacZ-sheets ($n = 5$) or NK4-sheets ($n = 5$) were implanted s.c. in an upside-down manner. In the control group ($n = 5$), mice were not treated after injection of cancer cells. Five mice of each experimental group were used for the tumor growth assessment. To quantify the tumor growth, two perpendicular diameters of the resultant s.c. tumors were measured with calipers every 3–5 days. The tumor volume was calculated using the formula: tumor volume (mm^3) = $0.52 \times$ [width (mm)]$^2 \times$ [length (mm)]. Another 11 mice were used for examination of angiogenesis (control, $n = 4$; lacZ-sheet, $n = 4$;

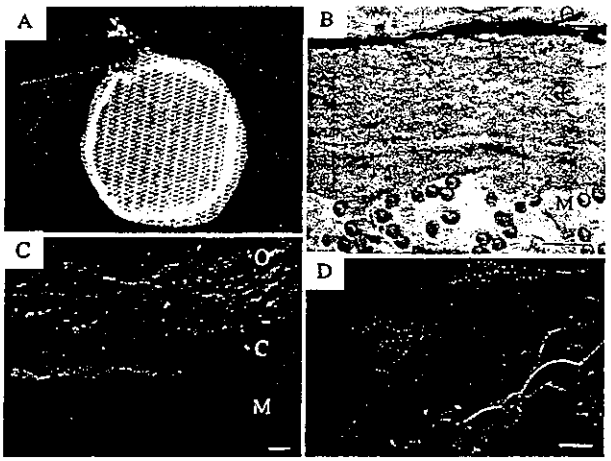

Fig. 2 OMEC sheet. *A*, gross appearance of OMEC sheet. *B*, H&E-stained cross-section of OMEC sheet. Bar, 50 μm. *C* and *D*, SEM of OMEC sheet (bar, 100 μm in *C* and 10 μm in *D*). The cells are polygonal and had regular microplicae. *O*, OMECs; *C*, collagen mesh; *M*, VICRYL mesh.

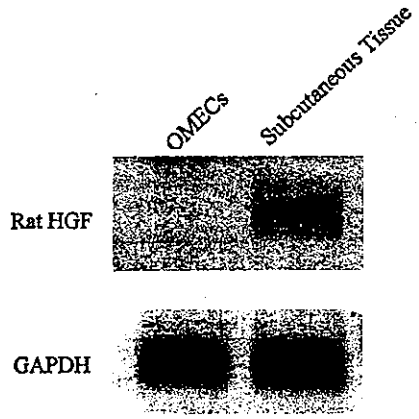

Fig. 3 Expression of HGF mRNA. RT-PCR was performed to examine whether OMECs expressed rat HGF mRNA. Rat HGF mRNA was detected in the s.c. tissue, which was used as a positive control. On the other hand, rat HGF mRNA was not detected in OMECs.

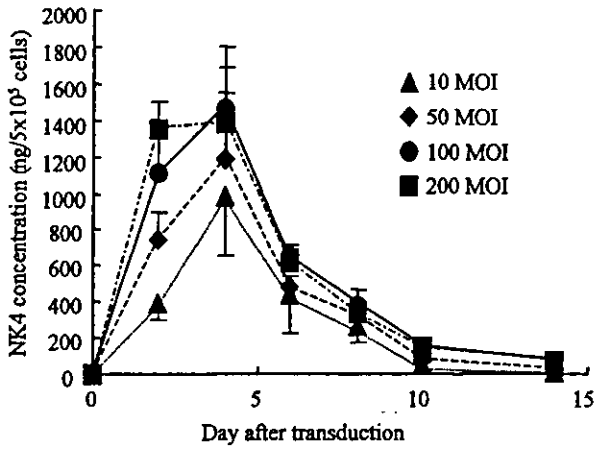

Fig. 4 Time course of the amount of NK4 secreted from Ad-NK4-transduced OMECs. OMECs were transduced with Ad-NK4 at different MOIs (MOI = 10, 50, 100, or 200). The amount of NK4 secreted in the medium was determined by ELISA every 2–4 days. Values are expressed as means ± SD (n = 3).

NK4-sheet, n = 3). Fourteen days after the injection of cancer cells, the tumor was removed and embedded in paraffin for immunohistochemical staining. Tissue sections were incubated with a rabbit polyclonal antibody against von Willebrand factor (DAKO Corp., Carpinteria, CA), and immunoreaction was visualized by staining with a 3,3′-diaminobenzidine-peroxidase complex (DAKO EnVision System; DAKO). The number of blood vessels was counted under a light microscope at ×200 magnification. At least 15 randomly selected fields were examined per section.

Statistical Analysis. Statistical analysis was performed with ANOVA. Post hoc comparisons were made by the Scheffe analysis. Differences were considered significant at $P < 0.05$.

RESULTS

Fabrication of OMEC Sheet. OMECs, which were harvested and cultured according to the 3T3 feeder layer technique (19–21), were seeded on the collagen mesh-overlayered VICRYL mesh to produce OMEC sheets. The gross appearance of the OMEC sheet after 3 days culture was thin and flexible (Fig. 2*A*). A phase-contrast microscopy image of a cross-section of an H&E-stained OMEC sheet showed that a monolayer of OMECs is formed on the collagen mesh (Fig. 2*B*). An SEM of the cross-section showed that the OMEC sheet was composed of three layers: (*a*) OMECs; (*b*) collagen mesh; and (*c*) the VICRYL mesh (Fig. 2*C*). OMECs cultured on collagen mesh were polygonal and had regular microplica similar to microridges with a cell membrane protrusion at the cell border as reported by Günter Lauer *et al.* (Fig. 2*D*; Ref. 31). To examine whether rat OMECs expressed rat HGF mRNA, RT-PCR was performed. The rat s.c. tissue showed a detectable level of rat HGF mRNA but not OMECs (Fig. 3).

Ad-NK4-transduced OMECs: *In Vitro* Release and Proliferation. OMECs were transduced with Ad-NK4 at an MOI of 10, 50, 100, and 200, and aliquots of supernatants were collected every 2 days and analyzed by ELISA (Fig. 4). The amount of NK4 secreted from Ad-NK4-transduced OMECs reached a maximal peak on day 4 and then gradually decreased, irrespective of MOI. The amount at the maximal peak was the highest at an MOI of 100–200. NK4 was not detected in supernatants of nontransduced OMECs and Ad-lacZ-transduced OMECs (data not shown). Ad-NK4 transduction was carried out at an MOI of 100 for additional experiments.

To examine the effect of Ad-NK4 on proliferation of OMECs, the proliferation profile of Ad-NK4-transduced OMECs was compared with those of nontransduced OMECs and Ad-lacZ-transduced OMECs (Fig. 5). Little statistical difference among them was observed within 48-h observation period. This indicates that neither viral transduction nor autocrine NK4 causes any significant effect on proliferation of OMECs.

Invasion Assay. To determine whether NK4 secreted from Ad-NK4-transduced OMECs inhibits the invasion of hu-

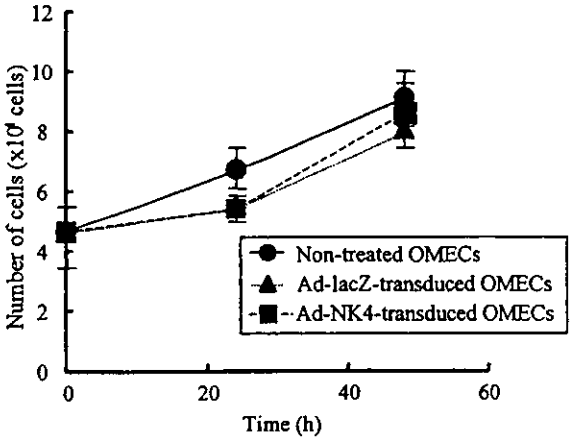

Fig. 5 Effect of Ad-NK4 on proliferation of OMECs. Proliferation characteristics of Ad-NK4-transduced OMECs (MOI = 100) were compared with those of nontreated OMECs and Ad-lacZ-transduced OMECs (MOI = 100). Values are expressed as means ± SD (n = 4). There were no significant differences among the three groups.

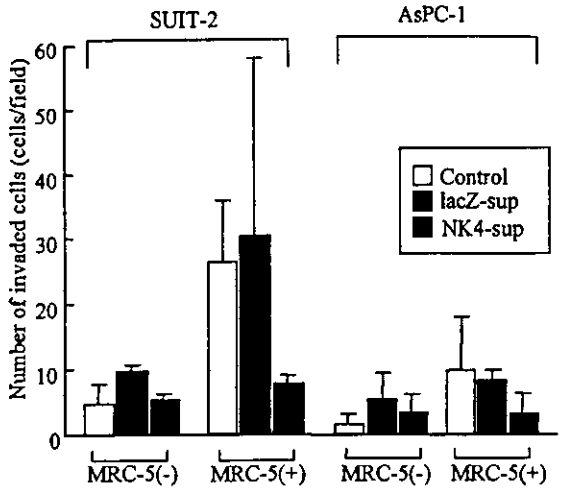

Fig. 6 Effect of NK4 secreted from Ad-NK4-transduced OMECs on invasion of human pancreatic cancer cells. In the presence of MRC-5, the numbers of invaded SUIT-2 cells cultured in the medium and lacZ-sup tended to be quite higher than those in the absence of MRC-5, whereas the number of invaded cells in NK4-sup was almost the same as that in the absence of MRC-5. For AsPC-1 cells, the same trend was observed. Values are expressed as means ± SD (n = 3).

man pancreatic cancer cells, an invasion assay was conducted using a Matrigel invasion chamber in the presence or absence of the cell-lined fibroblast that secretes HGF, MRC-5, in the outer cup of the chamber. The supernatant of Ad-NK4-transduced OMECs (NK4-sup), Ad-lacZ-transduced OMECs (lacZ-sup), or the medium (DMEM containing 2% FBS) was added into the inner cup that was preseeded with pancreatic cancer cells (SUIT-2 and AsPC-1). After 24-h cultivation, the number of the invaded cells, which were migrating to the opposite side of the filter membrane (average pore size, 8 μm) through the Matrigel, was counted. In the absence of MRC-5 in the outer cup, regardless of the type of cancer cell, there was little difference between the numbers of invaded cancer cells cultured in the medium, lacZ-sup, and NK4-sup. In the presence of MRC-5, the numbers of invaded SUIT-2 cells cultured in the medium and lacZ-sup tended to be quite higher than those in the absence of MRC-5, whereas the number of invaded cells in NK4-sup was almost the same as that in the absence of MRC-5. However, statistical difference was not significant. For AsPC-1 cells, the same trend was observed (Fig. 6).

i.m. Tumor Model with Adenoviral-transduced OMEC Sheet. OMEC sheets prepared from Ad-lacZ transduced OMECs (lacZ-sheet, MOI = 100) were implanted in an upside-down manner on established i.m. tumors composed of AsPC-1 cells. Four and 10 days after implantation, the tumors with surrounding tissues were resected. X-gal staining of cross-sections of tissues showed that the belt-like tissue of blue-stained cells (β-galactosidase-positive cells) along the collagen mesh was observed on day 4 (Fig. 7*A*), whereas only a small portion of blue-stained tissue was observed on day 10 (Fig. 7*B*).

To examine whether NK4 secreted from Ad-NK4-transduced OMEC sheet (NK4-sheet) was delivered into the tumor, NK4-sheets were implanted on established i.m. tumors, and after 4 days, the tumors were resected and subjected to ELISA. The amount of NK4 in the tumor lysate was 155.85 ± 60.83 ng/gram protein (n = 3), which remarkably decreased with time (8.36 ± 12.82 ng/gram protein at 7 days and 4.99 ± 6.99 ng/gram protein at 10 days; Table 1). On the other hand, in the tumors without the sheet or with lacZ-sheets, NK4 was undetectable. In the serum of mice implanted with NK4-sheets, NK4 was also undetectable. These results strongly indicate that NK4 secreted from the NK4-sheet permeated deeper into the target tissue and was delivered locally to a tumorous tissue.

Effect of NK4-Sheets on Growth and Angiogenesis of s.c. Tumors. NK4-sheets were implanted on the tumors 3 days after s.c. injection of AsPC-1 cells (3×10^6 cells/50 μl of DMEM), and we examined whether covering of the tumors with OMEC sheets affects the tumor growth. Separately, lacZ-sheets were also implanted in the same manner. The tumors with lacZ-sheets grew rapidly with time, the growth profile of which resembled that of the tumors without a sheet. On the other hand, the tumor growth was suppressed by covering with NK4-sheets (Fig. 8). To evaluate whether NK4-sheets affect angiogenesis, immunohistochemical staining of the tumors with von Willebrand factor was conducted 14 days after injection of AsPC-1 cells (11 days after implantation of NK4-sheets). The number of vessels of the tumors with NK4-sheets was significantly lower than those of the other two groups (Fig. 9). These results indicate that implantation of NK4-sheets near the tumors reduced the tumor growth rate, as well as inhibited angiogenesis of the tumors.

DISCUSSION

A series of our ongoing studies aimed at reducing retroperitoneal recurrence of pancreatic cancer is utilization of NK4, which has dual biological functions: an HGF antagonist and angiogenetic inhibitor. Our previous study has shown that the controlled release of these substances from photocured gelatinous matrix, which was adhered to a resected surface, was assessed using *in situ* photocured gelatinous matrix (16). The

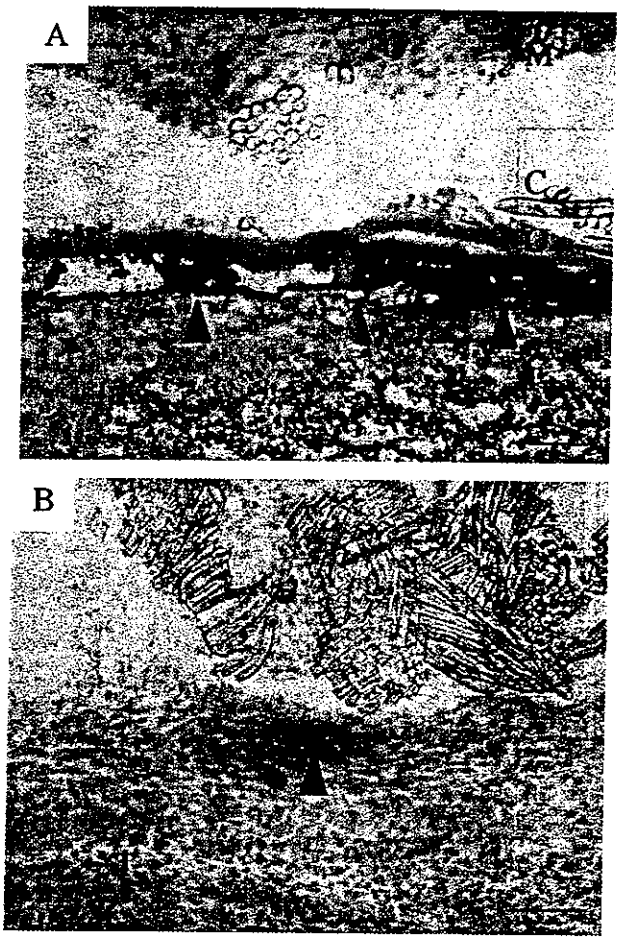

Fig. 7 Gene-transduced OMEC sheet in experimental tumor models. Cross-sectional image of Ad-lacZ-transduced OMEC sheet (lacZ-sheet) stained by X-gal and H&E. *A*, 4 days after implantation; *B*, 10 days after implantation. *Arrowheads*, X-gal-positive OMECs; bar, 100 μm. *O*, OMECs; *C*, collagenous gel; *M*, VICRYL mesh; *T*, tumor.

Table 1 Time course of the amount of NK4 in the tumors

Time course of the amounts of NK4 delivered from Ad-NK4-transduced OMEC sheets (NK4-sheets) into the tumors. Mice were sacrificed 4, 7, and 10 days after implantation of NK4 sheets. The amounts of NK4 in the tumor lysates were determined by ELISA. The tumors without the sheets (control) or with Ad-lacZ-transduced OMEC sheets were also examined on day 4 after implantation.

	Amount of NK4 (ng/gram protein)		
Group	4 day	7 day	10 day
Control	Undetectable	[a]	[a]
lacZ	Undetectable	[a]	[a]
NK4	155.86 ± 60.83	8.36 ± 12.82	4.99 ± 6.99

[a] Not examined.

sustainably released model protein could diffuse and be transported deep into the target tissue with time (Fig. 10*A*). The release rate and period were controlled by formulation parameters of a photocured gelatin solution and the porosity of photocured gelatinous matrix, which were reported in our previous

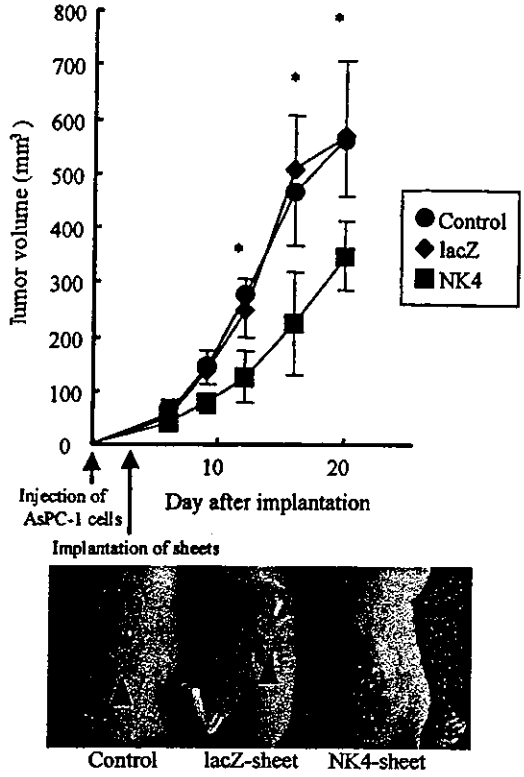

Fig. 8 Tumor growth of s.c. injected AsPC-1 cells. Three days after cancer cell injection, tumors were covered with lacZ-sheet or NK4-sheet. In the control group, mice were not treated. *A*, development of tumor arising from AsPC-1 cells. Values are expressed as means ± SD ($n = 5$, *; $P < 0.05$). *B*, gross appearance 14 days after AsPC-1 cell injection of each group.

study in detail. Because NK4 is available only for the experimental purpose at this time, the *NK4* gene-transduction method was devised in our previous study (17). However, when Ad-NK4 was immobilized into a photocured gelatinous matrix, Ad-NK4 diffused out from the matrix but was not transported into the target tissue (Fig. 10*B*). Because only cells present at the outermost surface of the target tissue were partially transduced, "passive"-diffusion-driven mechanism does not operate for a giant molecule, such as an adenovirus. As an alternative strategy for the therapy for local recurrence, we devised a cell-based protein delivery system, which was intraoperatively implanted with a gene-transduced cell-monolayer sheet as a vehicle for gene therapy.

For cell-based NK4 delivery, the selection of cell type used is essential. The requirement for a cell type is that such a cell does not inherently secrete HGF. Our survey experiment of mesenchymal cells as a possible candidate for a cell source showed that fibroblasts produced HGF at a relatively high level, and concomitantly, no suppressive effect of Ad-NK4-transduced fibroblasts on invasion of cancer cells was observed. On the other hand, autologous OMECs were found to be best suited to this purpose because of the following: (*a*) no secretion of HGF nor expression of HGF mRNA (Fig. 3); (*b*) reasonably high proliferation potential that is not affected by adenoviral transduction and NK4 (Fig. 5); (*c*) ease in harvesting from a patient;

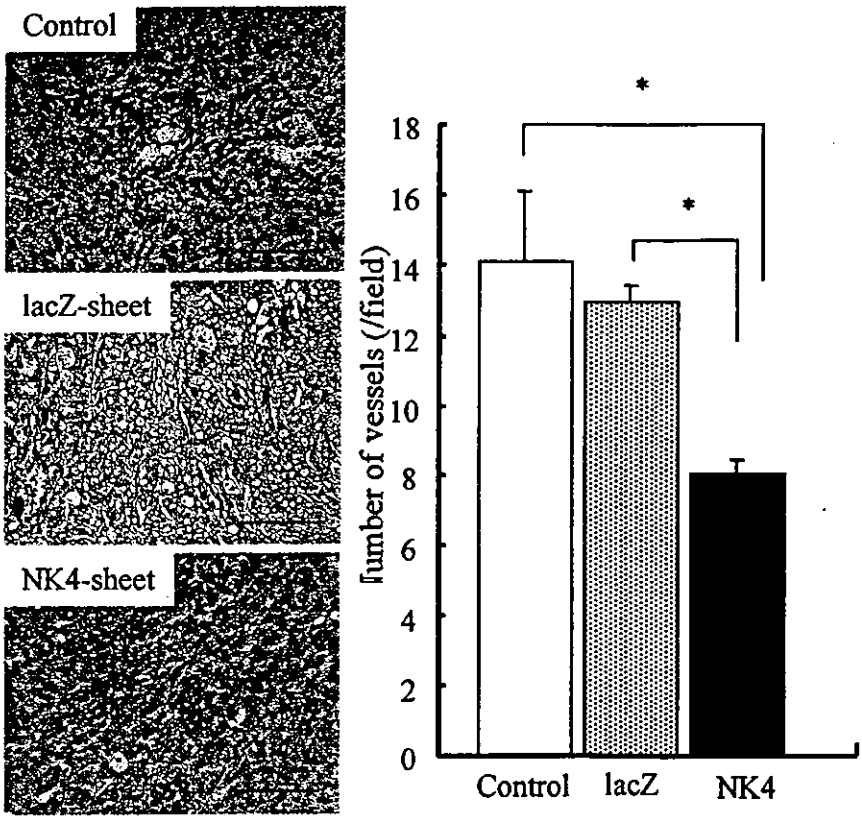

Fig. 9 Angiogenesis of tumors covered with Ad-NK4-transduced OMEC sheet in nude mice. Immunohistochemical staining of tumor tissues (control, $n = 4$; lacZ-sheet, $n = 4$; NK4-sheet, $n = 3$) for von Willebrand factor. Values are expressed as means ± SD (*; $P < 0.05$). *Bar*, 100 μm.

and (*d*) no immune reaction (19–21, 32, 33). Indeed, NK4 secreted from Ad-NK4-transduced OMECs suppressed invasion of pancreatic cancer cells, which was induced by MRC-5 *in vitro* (Fig. 6). Moreover, the proliferation of OMECs was not affected by viral transduction and autocrine NK4 (Fig. 5), although OMECs express c-Met receptor (33).

Our preliminary study using a prototype gene-transduced cell sheet indicated that heterotopically implanted gene-trans-

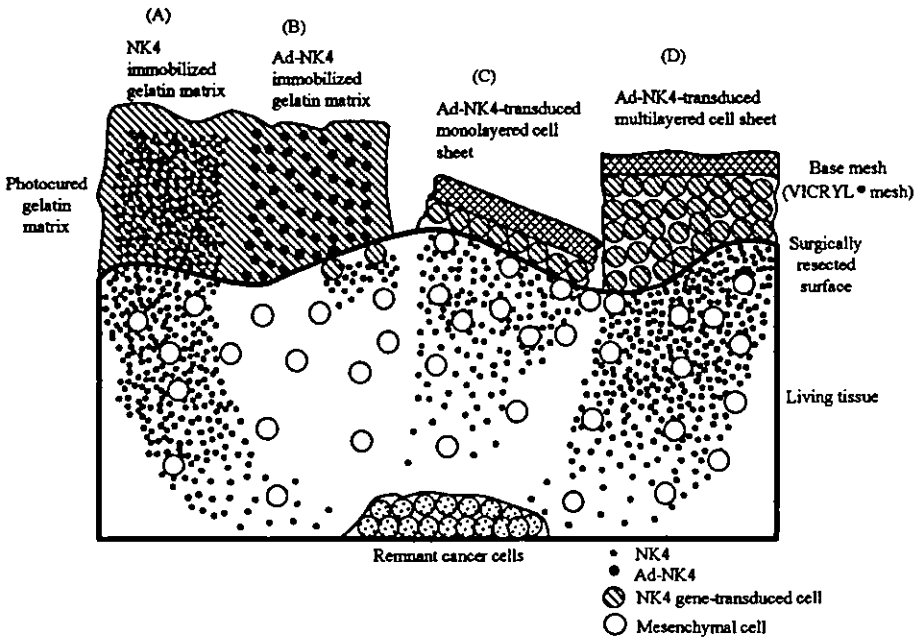

Fig. 10 Schematic of local protein delivery methods under development. *A*, NK4-immobilized photocured gelatinous matrix (16); *B*, Ad-NK4-immobilized photocured gelatinous matrix (17); *C*, Ad-NK4-transduced monolayered cell sheet (present study); *D*, Ad-NK4-transduced multilayered cell sheet.

duced OMECs remained for ≥10-day observation period, and NK4 was delivered into the tumor by Ad-NK4-transduced OMEC sheets, although gene expression significantly decreased with time. One possible reason for the decrease in gene expression was transient expression of adenoviral transduction. Despite a low level of NK4 delivery from Ad-NK4-transduced OMEC sheets into the tumor, these sheets inhibited angiogenesis and tumor growth (Figs. 7 and 8). However, the tumor growth gradually increased with time, which must be attributable to a time-dependent decrease in the amount of NK4. The antiangiogenic effect observed in this study was also observed in our previous studies, which were verified by i.p. injection or intratumoral injection of NK4 or Ad-NK4 (9, 12–15).

In conclusion, Ad-NK4-transduced OMECs, from which secreted NK4 diffuses into a tumor tissue (Fig. 10*A*), appear to offer a new therapeutic modality for local recurrence of pancreatic cancer. The shortcomings of a prototype technology, such as the low level and short period of NK4 production, may be overcome by high density seeding of gene-transduced cells, *e.g.*, multilayering on a microporous matrix as schematically shown in Fig. 10*D*. It is highly envisaged that the combination of a high cell seeding and more powerful vector enabling longer term NK4 secretion, such as retrovirus vectors, overcome the shortcomings of the prototype cell-sheet device in this study. On the basis of such a hypothesis-driven strategy, we may offer a new therapeutic choice to improve the survival of pancreatic cancer patients.

ACKNOWLEDGMENTS

We thank K. Yasutake and E. Koga for excellent technical assistance, H. Okino for technical advice, and T. Kanemaru for scanning electron examination.

REFERENCES

1. Cienfuegos, J. A., and Manuel, F. A. Analysis of intraoperative radiotherapy for pancreatic carcinoma. Eur. J. Surg. Oncol., *26:* S13–S15, 2000.

2. Takeda, S., Inoue, S., Kaneko, T., Harada, A., and Nakao, A. The role of adjuvant therapy for pancreatic cancer. Hepatogastroenterology, *48:* 953–956, 2001.

3. Jiang, W., Hiscox, S., Matsumoto, K., and Nakamura, T. Hepatocyte growth factor/scatter factor, its molecular, cellular and clinical implications in cancer. Crit. Rev. Oncol. Hematol., *29:* 209–248, 1999.

4. Matsumoto, K., and Nakamura, T. HGF-c-Met receptor pathway in tumor invasion-metastasis and potential cancer treatment with NK4. *In:* W. G. Jiang, K. Matsumoto, and T. Nakamura (eds), Growth Factors and Their Receptors in Cancer Metastasis, pp. 241–276. Kluwer Academic Publisher: NY, 2001.

5. Date, K., Matsumoto, K., Kuba, K., Shimura, H., Tanaka, M., and Nakamura, T. Inhibition of tumor growth and invasion by a four-kringle antagonist (HGF/NK4) for hepatocyte growth factor. Oncogene, *17:* 3045–3054, 1998.

6. Date, K., Matsumoto, K., Shimura, H., Tanaka, M., and Nakamura, T. HGF/NK4 is a specific antagonist for pleiotrophic actions of hepatocyte growth factor. FEBS Lett., *420:* 1–6, 1997.

7. Kuba, K., Matsumoto, K., Ohnishi, K., Shiratsuchi, T., Tanaka, M., and Nakamura, T. Kringle 1–4 of hepatocyte growth factor inhibits proliferation and migration of human microvascular endothelial cells. Biochem. Biophys. Res. Commun., *279:* 846–852, 2000.

8. Kuba, K., Matsumoto, K., Date, K., Shimura, H., Tanaka, M., and Nakamura, T. HGF/NK4, a four-kringle antagonist of hepatocyte growth factor, is an angiogenesis inhibitor that suppresses tumor growth and metastasis in mice. Cancer Res., *60:* 6737–6743, 2000.

9. Maehara, N., Matsumoto, K., Kuba, K., Mizumoto, K., Tanaka, M., and Nakamura, T. NK4, a four-kringle antagonist of HGF, inhibits spreading and invasion of human pancreatic cancer cells. Br. J. Cancer, *84:* 864–873, 2001.

10. Di Renzo, M. F., Poulsom, R., Olivero, M., Comoglio, P. M., and Lemoine, N. R. Expression of the Met/hepatocyte growth factor receptor in human pancreatic cancer. Cancer Res., *55:* 1129–1138, 1995.

11. Ebert, M., Yokoyama, M., Friess, H., Buchler, M. W., and Korc, M. Coexpression of the c-met proto-oncogene and hepatocyte growth factor in human pancreatic cancer. Cancer Res., *54:* 5775–5778, 1994.

12. Maehara, N., Nagai, E., Mizumoto, K., Sato, N., Matsumoto, K., Nakamura, T., Narumi, K., Nukiwa, T., and Tanaka, M. Gene transduction of NK4, HGF antagonist, inhibits in vitro invasion and in vivo growth of human pancreatic cancer. Clin. Exp. Metastasis, *19:* 417–426, 2002.

13. Tomioka, D., Maehara, N., Kuba, K., Mizumoto, K., Tanaka, M., Matsumoto, K., and Nakamura, T. Inhibition of growth, invasion, and metastasis of human pancreatic carcinoma cells by NK4 in an orthotopic mouse model. Cancer Res., *61:* 7518–7524, 2001.

14. Saimura, M., Nagai, E., Mizumoto, K., Maehara, N., Okino, H., Katano, M., Matsumoto, K., Nakamura, T., Narumi, K., Nukiwa, T., and Tanaka, M. Intraperitoneal injection of adenovirus-mediated NK4 gene suppresses peritoneal dissemination of pancreatic cancer cell line AsPC-1 in nude mice. Cancer Gene Ther., *9:* 799–806, 2002.

15. Saimura, M., Nagai, E., Mizumoto, K., Maehara, N., Minamishima, Y. A., Katano, M., Matsumoto, K., Nakamura, T., and Tanaka, M. Tumor suppression through angiogenesis inhibition by SUIT-2 pancreatic cancer cells genetically engineered to secrete NK4. Clin. Cancer Res., *8:* 3243–3249, 2002.

16. Okino, H., Nakayama, Y., Tanaka, M., and Matsuda, T. In situ hydrogelation of photocurable gelatin and drug release. J. Biomed. Mater. Res., *59:* 233–245, 2002.

17. Okino, H., Manabe, T., Tanaka, M., and Matsuda, T. Novel therapeutic strategy for prevention of malignant tumor recurrence after surgery: local delivery and prolonged release of adenovirus immobilized in photocured, tissue-adhesive gelatinous matrix. J. Biomed. Mater. Res., in press.

18. Jain, R. K. Barriers to drug delivery in solid tumors. Sci. Am., *271:* 58–65, 1994.

19. Ueda, M., Hata, K., Horie, K., and Torii, S. The potential of oral mucosal cells for cultured epithelium: a preliminary report. Ann. Plast. Surg., *35:* 498–504, 1995.

20. Hata, K., Kagami, H., Ueda, M., Torii, S., and Matsuyama, M. The characteristics of cultured mucosal cell sheet as a material for grafting; comparison with cultured epidermal cell sheet. Ann. Plast. Surg., *34:* 530–538, 1995.

21. Rheinwald, J. G., and Green, H. Serial cultivation of strains of human epidermal keratinocytes: the formation of keratinizing colonies from single cells. Cell, *6:* 331–343, 1975.

22. Sun, W., Funakoshi, H., and Nakamura, T. Differential expression of hepatocyte growth factor and its receptor, c-Met in the rat retina during development. Brain Res., *851:* 46–53, 1999.

23. Chen, W. H., Horoszewicz, J. S., Leong, S. S., Shimano, T., Penetrante, R., Sanders, W. H., Berjian, R., Douglass, H. O., Martin, E. W., and Chu, T. M. Human pancreatic adenocarcinoma: in vitro and in vivo morphology of a new tumor line established from ascites. In Vitro, *18:* 24–34, 1982.

24. Iwamura, T., Katsuki, T., and Ide, K. Establishment and characterization of a human pancreatic cancer cell line (SUIT-2) producing carcinoembryonic antigen and carbohydrate antigen 19–9. Tissue Eng., *78:* 54–62, 1987.

25. Li, J. J., Ueno, H., Tomita, H., Yamamoto, H., Kanegae, Y., Saito, I., and Takeshita, A. Adenovirus-mediated arterial gene transfer does not require prior injury for submaximal gene expression. Gene Ther., *2:* 351–354, 1995.

26. Li, J. J., Ueno, H., Pan, Y., Tomita, H., Yamamoto, H., Kanegae, Y., Saito, I., and Takeshita, A. Percutaneous transluminal gene transfer into canine myocardium in vivo by replication-defective adenovirus. Cardiovasc. Res., *30:* 97–105, 1995.

27. Horch, R. E., Debus, M., Wagner, G., and Stark, G. B. Cultured human keratinocytes on type I collagen membranes to reconstitute the epidermis. Tissue Eng., *6:* 53–67, 2000.

28. Matouskova, E., Bucek, S., Vogtova, D., Vesely, P., Chaloupkova, A., Broz, L., Singernova, H., Pavlikova, L., and Konigova, R. Treatment of burns and donor sites with human allogeneic keratinocytes grown on acellular pig dermis. Br. J. Dermatol., *136:* 901–907, 1997.

29. Takeda, T., Tanaka, H., Matsuda, H., and Shimazaki, S. Enzyme-free method for cultured skin grafting. J. Investig. Surg., *12:* 125–127, 1999.

30. Hashimoto, M., Aruga, J., Hosoya, Y., Kanegae, Y., Saito, I., and Mikoshiba, K. A neural cell-type-specific expression system using recombinant adenovirus vectors. Hum. Gene Ther., *7:* 149–158, 1996.

31. Lauer, G., Otten, J. E., von Specht, B. U., and Schilli, W. Cultured gingival epithelium. A possible suitable material for pre-prosthetic surgery. J. Craniomaxillofac. Surg., *19:* 21–26, 1991.

32. Sato, C., Tsuboi, R., Shi, C. M., Rubin, J. S., and Ogawa, H. Comparative study of hepatocyte growth factor/scatter factor and keratinocyte growth factor effects on human keratinocytes. J. Investig. Dermatol., *104:* 958–963, 1995.

33. Bennett, J. H., Morgan, M. J., Whawell, S. A., Atkin, P., Roblin, P., Furness, J., and Speight, P. M. Metalloproteinase expression in normal and malignant oral keratinocytes: stimulation of MMP-2 and -9 by scatter factor. Eur. J. Oral Sci., *108:* 281–291, 2000.

Available online at www.sciencedirect.com

SCIENCE DIRECT

Journal of Controlled Release 100 (2004) 317–330

journal of controlled release

www.elsevier.com/locate/jconrel

Review

Novel strategic therapeutic approaches for prevention of local recurrence of pancreatic cancer after resection: trans-tissue, sustained local drug-delivery systems

Tatsuya Manabe[a,b], Hidenobu Okino[a,b], Ryo Maeyama[a,b], Kazuhiro Mizumoto[b], Eishi Nagai[b], Masao Tanaka[b], Takehisa Matsuda[a,*]

[a]*Division of Biomedical Engineering, Graduate School of Medicine, Kyushu University, 3-1-1 Maidashi, Fukuoka 812-8582, Japan*
[b]*Division of Surgery and Oncology, Graduate School of Medicine, Kyushu University, 3-1-1 Maidashi, Higashi-ku, Fukuoka 812-8582, Japan*

Received 27 May 2004; accepted 15 September 2004
Available online 19 October 2004

Abstract

Local recurrence and hepatic metastasis are still the major causes of death of patients who have undergone resection for pancreatic cancer. To decrease the incidence of local recurrence, we have proposed and devised several trans-tissue and local delivery systems, all of which could be applied immediately after surgery at the resected sites: (1) System I: a drug-loaded photocured gelatinous tissue-adhesive gel (bioactive substance reservoir) that enables the sustained release of a drug, protein, or gene-encoding adenovirus, (2) System II: an anti-cytokine antibody-fixed photocured gelatinous, tissue-adhesive gel (cytokine barrier) that prevents cytokine permeation into the resected tissue, (3) System III: a gene-modified cell sheet that enables the sustained release of a very costly protein produced by gene-transduced cells and (4) System IV: a percutaneous drug-delivery device that enables continuous drug infusion and easy removal from the body. This review article is a summary of our several years of efforts and attempts, which are composed of integrated disciplines including active biomaterials and genetic- and tissue-engineerings, to overcome the recurrence of pancreatic cancer. Here, we outline our proposed strategies and therapeutic devices/materials and discuss their potential therapeutic effectiveness, promises and challenges in the clinical settings.

Keywords: Local drug delivery; Pancreatic cancer; Local recurrence; Cytostasic therapy; Cytocidal therapy

* Corresponding author. Tel.: +81 92 642 6211; fax: +81 92 642 6212.
E-mail address: matsuda@med.kyushu-u.ac.jp (T. Matsuda).

0168-3659/$ - see front matter © 2004 Elsevier B.V. All rights reserved.
doi:10.1016/j.jconrel.2004.09.007

Contents

1. Introduction

Surgical resection is the first and most effective therapeutic choice for pancreatic cancer that is localized without distant metastases. Although extended surgery with portal vein resection has been attempted, the survival rate for patients who have undergone resection for pancreatic cancer is still very low (8–25%) [1–4]. One reason is that pancreatic cancer cells, which easily invade and develop into the extrapancreatic nerve plexus and lymph vessels, remain in the pancreatic bed (the retroperitoneal space) even after curative resection, and subsequently induce local recurrence at a high incidence [5–8]. Intraoperative radiotherapy as an adjuvant treatment has been used to try to reduce local recurrence, but its effectiveness is still under debate [9–11]. When detected clinically, local recurrence is mostly difficult to treat, because it occurs at a deep area in the body and has already established a tumor mass, which has physiological and environmental resistance to chemotherapy and radiotherapy [12,13]. The most critical timing of treatment for the prevention of local recurrence must be immediately after resection during surgery, prior to tumor mass formation derived from remnant cancer cells.

Regarding the environment of remnant cancer cells after surgery, surgical wounds induce inflammation and regeneration of tissues with an increased level of cytokines that provides favorable conditions for tumor recurrence [14–17]. That is, cytokines, which are produced and exist in a tumor-resected tissue and in the intraperitoneal space due to surgical trauma, such as hepatocyte growth factor (HGF), epidermal growth factor (EGF), basic fibroblast growth factor (bFGF), transforming growth factor-β (TGF-β) and vascular endothelial growth factor (VEGF), accelerate cancer cell proliferation, migration, invasion and tumor angiogenesis, resulting in recurrence and metastasis of cancer (Fig. 1). This is a well-accepted scenario of recurrence of pancreatic cancer.

To suppress the progress of cancer cells, there must be two main strategies; one is cytostatic therapy using a cytokine antagonist or an anti-cytokine antibody, and the other is cytocidal therapy using anticancer drugs or radiotherapy (Fig. 1) [18]. The goal of cytostatic therapy is to suppress cancer cell proliferation, migration, invasion and tumor angiogenesis, thus generating to a state of dormancy, while cytocidal therapy is aimed at a measurable reduction in tumor bulk. Regardless of cytostatic or cytocidal drugs, most of these drugs have been applied systemically via oral administration or intravenous injection. However, a complete cure has rarely been seen, and some severe adverse effects have been reported [19].

To achieve the markedly elevated pharmacological effect while minimizing systemic administration-associated toxic adverse effect, we have proposed and devised several trans-tissue and local delivery systems as shown below, all of which are processed to be tightly adhered or fixed on the resected tissues during surgery:

(1) System I: a drug-loaded photocured gelatinous tissue-adhesive gel (bioactive substance reser-

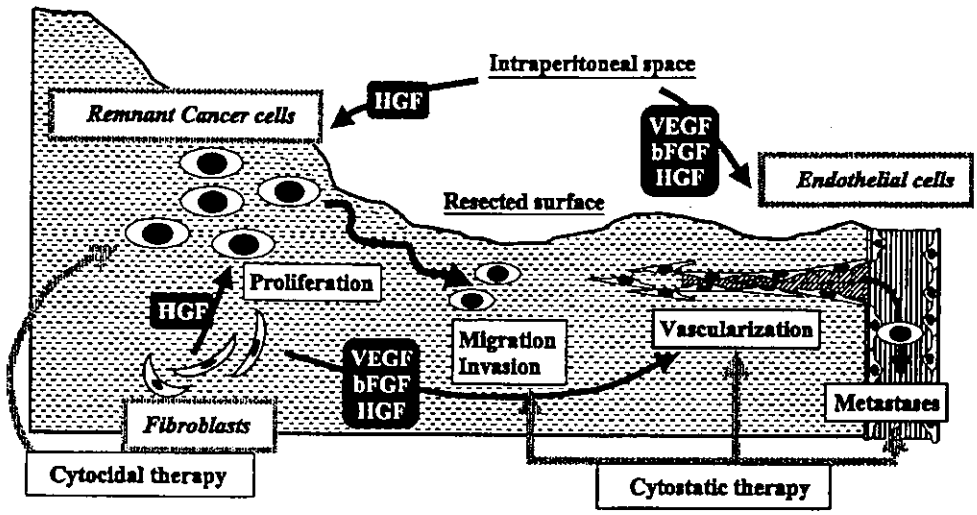

Fig. 1. Schematic of the progression of remnant cancer cells after surgery and relations with cytocidal and cytostatic therapies.

voir) that enables sustained release of a drug, protein, or gene-encoding adenovirus [20–22].

(2) System II: an anti-cytokine antibody-fixed photocured gelatinous, tissue-adhesive gel (cytokine barrier) that prevents cytokine permeation into the target tissue [23].

(3) System III: a gene-modified cell sheet that enables the sustained release of a very costly protein produced by gene-transduced cells [24].

(4) System IV: a percutaneous drug-delivery device that enables continuous drug infusion and easy detachment from the surgical site [25].

All the systems could be applicable for resected surfaces immediately after surgery (Fig. 2). The trans-tissue, local delivery systems devised have clear-cut advantages, including a high local concentration of drugs at the target tissue and a relatively low concentration at systemic organs, resulting in significant enhancement of the therapeutic effect of drugs and a marked reduction of systemic adverse effects.

In our studies [20–25], HGF antagonist, NK4, was used as a cytostatic drug. HGF plays an important role in tumor–stroma interaction and acts as a potent scattering factor by binding to c-Met

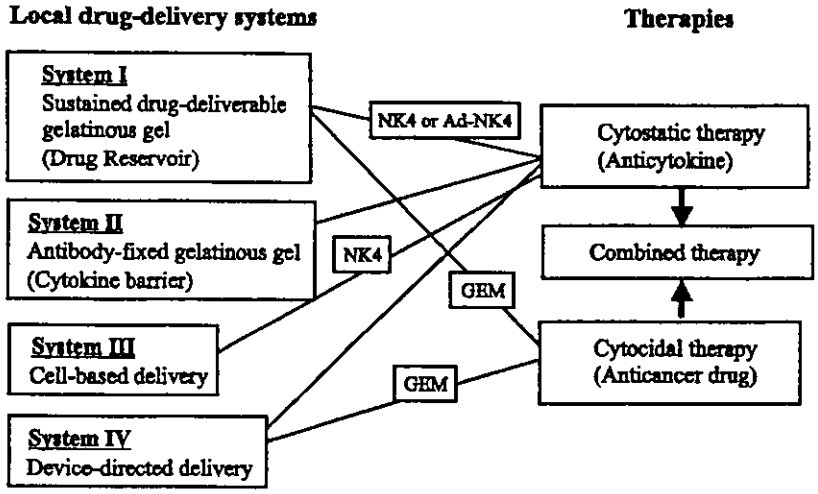

Fig. 2. Strategies for the prevention of local recurrence. NK4 is a cytostatic drug, which acts as a HGF antagonist and an angiogenic inhibitor. Gemcitabine (GEM) is a cytocidal drug, which acts as an antimetabolite [20–24].

receptor, which is frequently overexpressed in pancreatic cancers. NK4, composed of the N-terminal hairpin and four kringle domains of the α-subunit of HGF, binds to the c-Met receptor without tyrosine phosphorylation of c-Met, resulting in the inhibition of the mitogenic, motogenic and morphogenic activities of HGF [26–30]. Furthermore, NK4 acts as an angiogenic inhibitor, which inhibits the growth and migration of endothelial cells stimulated by VEGF, bFGF and HGF [31,32].

On the other hand, as a cytocidal drug, gemcitabine (2′,2′-difluorodeoxycitidine, GEM) was used. GEM, which inhibits DNA synthesis by the inhibition of ribonucleotide reductase and by its incorporation into DNA [33,34], is currently the most effective chemotherapeutic drug for pancreatic cancer. Several investigators reported that the cytocidal efficacy of GEM, which is an antimetabolite, increases with the exposure time [35–38].

This review article is a summary of our several years of efforts and attempts to overcome the recurrence of pancreatic cancer, and we outline our proposed strategies and discuss their promises and challenges in the clinical setting.

2. System I: drug-loaded gelatinous gel [20–22]

This system was developed to provide an in situ-formed locally deliverable gelatinous matrix that could adhere to the resected tissues, from which bioactive substances including drugs, proteins or gene-encoding adenoviruses can be sustainably released into the target tissue. To meet the desired performance in this particular application, the system should have the following characteristic features: (1) rapid sol-to-gel transformation by visible light photoirradiation, (2) strong tissue adhesivity, (3) ease of drug immobilization, (4) biodegradability and biosorption (5) minimal or very mild informatory reaction. To this end, photopolymerizable gelatin, which is partially derivatized with styrene groups in gelatin molecule (ST-gelatin; Fig. 3A), was used as an in situ gelable drug-loadable matrix. ST-gelatin was originally prepared at our laboratory as a visible light-induced photocurable tissue-adhesive glue, which prevented bleeding from arteries, indicating that such a glue inherently has a high tissue adhesivity, causes minimal inflammatory reaction and exhibits little sign of toxicity [39].

A viscous buffer solution composed of ST-gelatin, water-soluble carboxylated camphorquinone (visible light-induced radical generator used in clinical dental applications for many years), and the drug of interest was coated on resected tissues and photoirradiated with a visible light lamp (used in clinical dental applications), resulting in gel formation within 3 min of irradiation (Fig. 3B). The viscosity, in situ gelation time, drug-release rate, adhesive strength, and biodegradability were easily controlled by material (degree of derivatization of styrene groups in a gelatin molecule), formulation (concentrations of ST-gelatin and camphorquinone), and operation (photointensity and irradiation time) variables [20]. The general trend is that higher concentration of ST-gelatin, longer

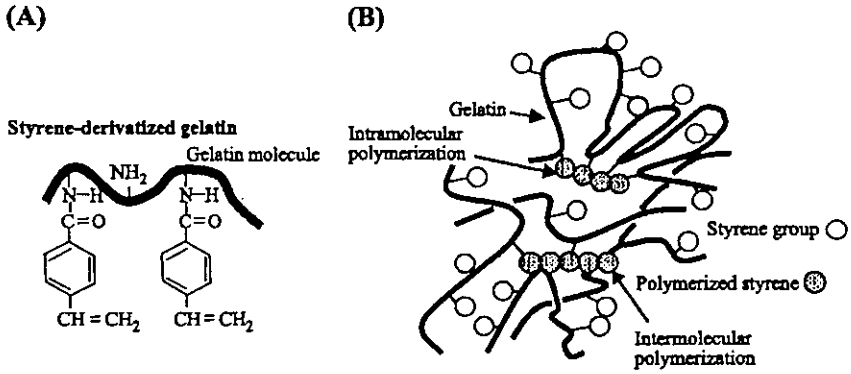

Fig. 3. Drug-loadable photocurable tissue-adhesive matrix. (A) Chemical structure of styrene-derivatized gelatin. (B) Photogelation by formation of cross-linked gelatin networks by the inter- and intra-molecular polymerizations of styrene groups in gelatin molecules.

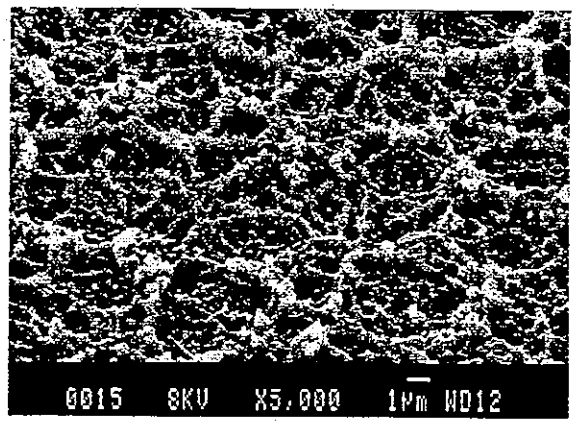

Fig. 4. Scanning electron micrograph of the beads-necklace type-surface of photocured ST-gelatin gel. Gelatin concentration: 30 wt.%. Bar: 1 μm [20].

photoirradiation time or higher photointensity produces a less water-swellable gel.

The formed gel consisted of supramolecular organization of polymerized gelatin with polymorphous nanostructures, which depends on the concentration of ST-gelatin and the degree of derivatization of styrene group in a gelatin molecule. The typical beaded necklace-type mesh appearance is shown in Fig. 4. The polymorphous nanostructured meshes or sheets of polymerized ST-gelatin are shown in Fig. 5. The general observation is that at low concentration of ST-gelatin, nanoparticles (diameter: approximately 100 nm) are adhered for each other to form continuous bead network with ample open-cell microvoids or channels (Fig. 5A1). Increased concentration of ST-gelatin produced beaded necklace-type mesh with a lesser degree of microvoids (Fig. 5A2). At high concentration, beads or necklace were fused to form a microporous continuous dense sheet (Fig. 5A3). In addition to the concentration of ST-gelatin, this tendency was enhanced with a lower degree of styrene derivatization (Fig. 5B). Such morphological features correlated well with the swellability of gel in water: Lower microvoid, lesser swellability. This in turn means that morphological features eventually determine the releasing profile of drug immobilized in a gel as shown below.

The typical time-dependent release profile of protein is a fast release in an early period, followed by reduced releasing characteristics (Fig. 6). The releasing rate of a proteinaceous drug was enhanced with a higher degree of swelling in water and with lower degree of derivatization of styrene in gelatin. The diffusion constants, calculated using Fick's second law, largely depended on the swellability of gels, which depends on the concentration of ST-gelatin (Fig. 7). The releasing period can be extended

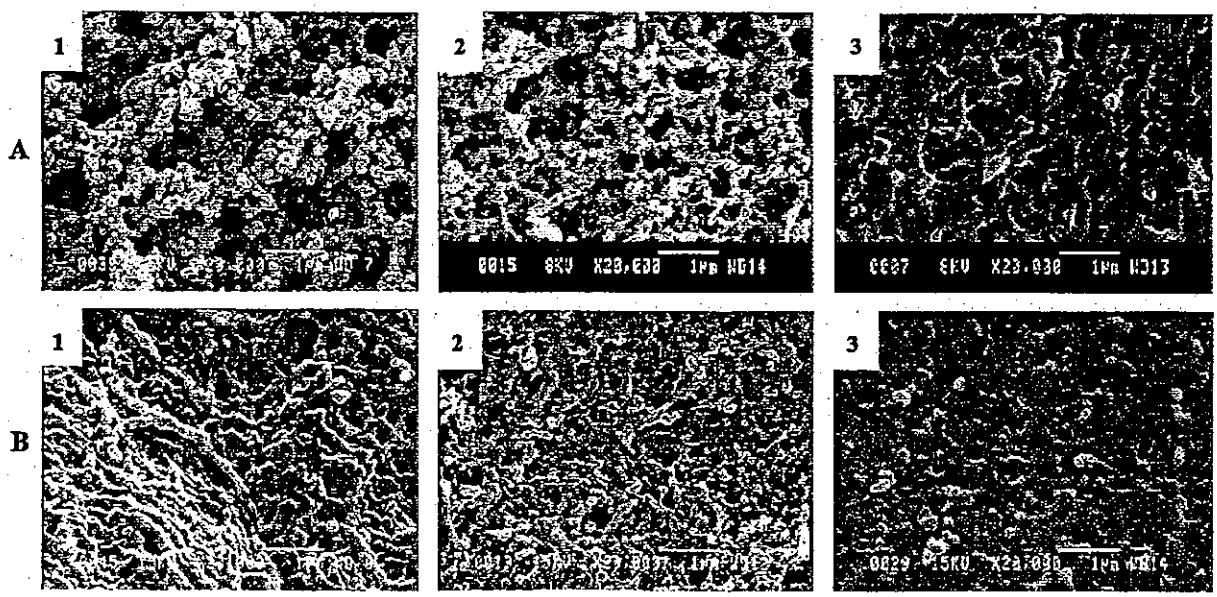

Fig. 5. Scanning electron micrographs of polymorphorous surfaces of photocured gelatins with variable concentration and variable styrene content in a gelatin molecule. Stryene content per molecule; 28.5 (A) and 22.4 (B). ST-gelatin content; 10 wt.% (1), 20 wt.% (2) and 40 wt.% (3). Bar: 1 μm.

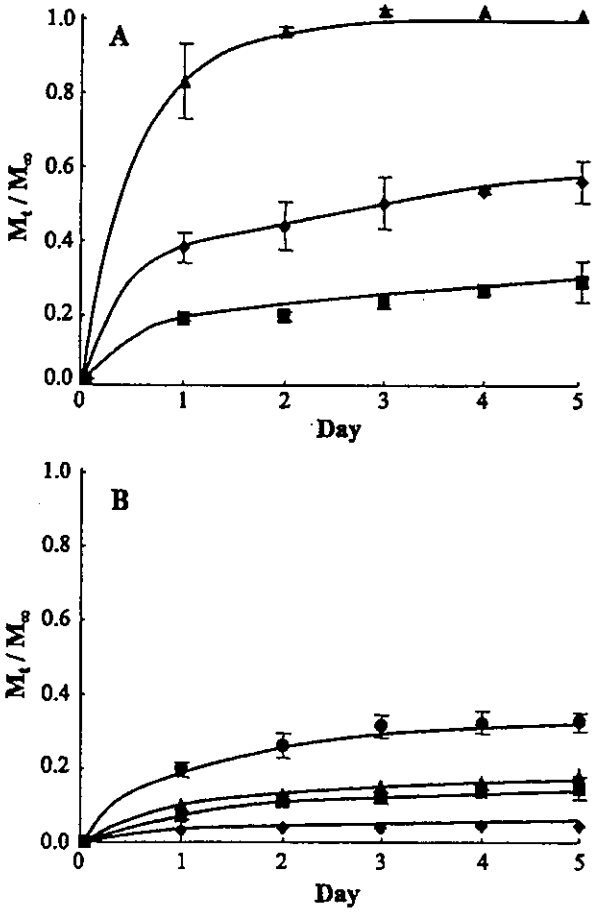

Fig. 6. Fraction release of rhodamine-albumin (r-Alb) as a function of time. Gel containing 10 wt.% (●), 20 wt.% (▲), 30 wt.% (■) and 50 wt.% (♦) of ST-gelatin of different contents of styrene per molecule (4.0 for A and 17.7 for B).

from days to several weeks, depending on the degree of photocuring or swellability of a formed gel. Fig. 8 shows the schematic of process of photogel formation and subsequent release of bioactive substances (A: drug, B: gene-encoding adenovirus) and experimental gel formation model using resected liver tissue (C). The followings are examples in System I loaded with bioactive substances.

2.1. NK4 [20]

The strategy for NK4 protein (MW; 64 000 g/mol) delivery is that an NK4-mixed ST-gelatin solution is photogelled on a target tissue where remnant cancer cells might remain, and NK4 released from the gel permeates gradually into the tissue, resulting in the suppression of cancer progression (Fig. 8A). The in vitro release profile of rhodamine-conjugated albumin (r-Alb, MW; 66 000 g/mol, used as a model protein of NK4) from ST-gelatin gel was characterized by an initial burst and subsequent gradual release over a prolonged period. In an in vivo experiment, 3 days after an r-Alb-loaded ST-gelatin solution was photogelled on the liver of a Wistar rat (Fig. 8C), r-Alb released from the gel remained in the liver from the surface to the deeper portions of the liver tissue. When NK4 is commercially manufactured at a low price, the prospective use of this system is very high. However, at present, NK4 is available only for experimental use in limited amounts so that it is doubtful that this system will be used in clinical situations in the near future.

2.2. NK4 gene-encoding adenovirus (Ad-NK4) [21]

Ad-NK4 is released from a photocured gelatinous gel formed on the tissue, and gradually permeates into the tissue, followed by transduction into various types of cells in the target tissue. Consequently, transduced cells produce NK4 (Fig. 8B). Although it is anticipated that the sustained release of an adenovirus might overcome the transient gene expression following adenoviral transduction, the amount of in vivo gene expression was substantially lower than that following simple injection of Ad-lacZ solution (Fig. 9A), probably because the adenoviral vector particles are too large to permeate the tissue via passive diffusion from the gel. In fact, our extensive study of gene transduction in rat's liver and muscle tissues showed

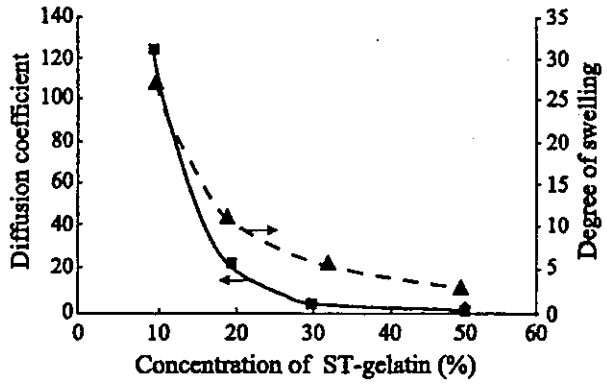

Fig. 7. Dependence of diffusion coefficient (■) and water swellability (▲) on concentration of ST-gelatin. Diffusion coefficient was obtained from the slope of the linear relation between M_t/M_∞ and $t^{1/2}$.

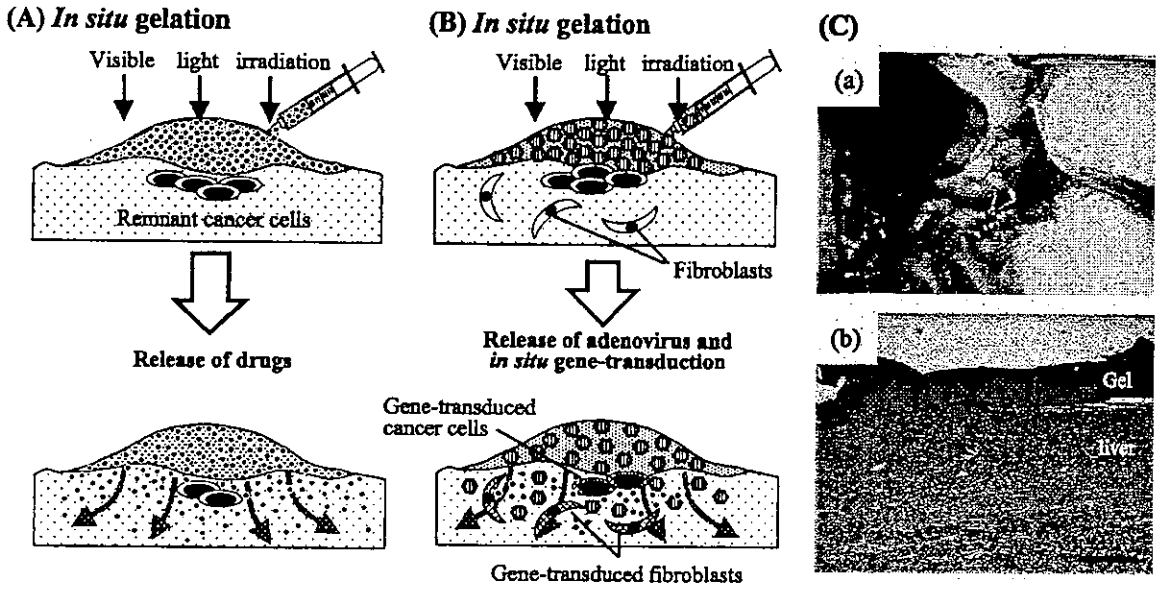

Fig. 8. Schematic of sustained drug-deliverable gelatinous gel (System I). (A) Local delivery of NK4 or Gemcitabine using photocurable gelatin. NK4- or Gemcitabine-loaded photocurable gelatin is coated on a tumor bed, and subsequently in situ photogelled under visible light irradiation. NK4 or Gemcitabine is released from the gel, and permeates into the tumor bed. (B) Local delivery of Ad-NK4 using photocurable gelatin. Ad-NK4-loaded photocurable gelatin is administered on a tumor bed, and subsequently in situ photogelled under visible light irradiation. Ad-NK4 is released from the gel, permeates into the tumor bed and transduces various cells around the tumor bed. Gene-transduced cells produce NK4. Irrespective of models, the inhibition of the progression of remnant cancer cells is expected. (C) In situ production of photocurable gelatin gel. (a) Procedure of visible-light irradiation of the aqueous gelatin solution on the liver surface. Gel formed on the liver surface. (b) Cross-sectional specimen (hematoxylin-and-eosin staining). Bar: 500 μm [20–22].

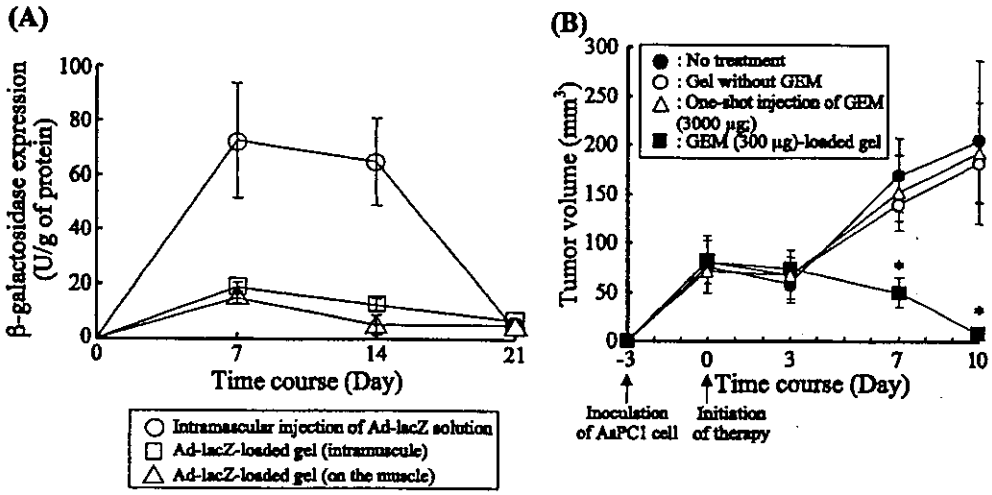

Fig. 9. (A) System I loaded with gene-encoding adenovirus. Time course of in vivo β-galactosidase expression in rat femoral muscle using Ad-lacZ-loaded gelatinous gel: One-shot intramuscular injection of Ad-lacZ solution (1.25×10^8 PFU/500 μl, ○), intramuscular injection of Ad-lacZ-loaded gel (1.25×10^8 PFU/500 μl, □), and covering on the muscle of Ad-lacZ-loaded gel (1.25×10^8 PFU/500 μl, △). The expression with the gel was lower than that of one-shot injection. Values are shown as means±S.D. (three mice/each group). (B) System I loaded with GEM. Effect of GEM-loaded photocured gelatinous gel on tumor growth of pancreatic cell line AsPC-1: no treatment (●), gel without GEM (○), one-shot injection of GEM (3000 μg; △), GEM (300 μg)-loaded gel (■). Values are shown as means±S.D. (10 mice/each group). The tumor volume with GEM-loaded gel was compared with that with the others (*P<0.01) [22].

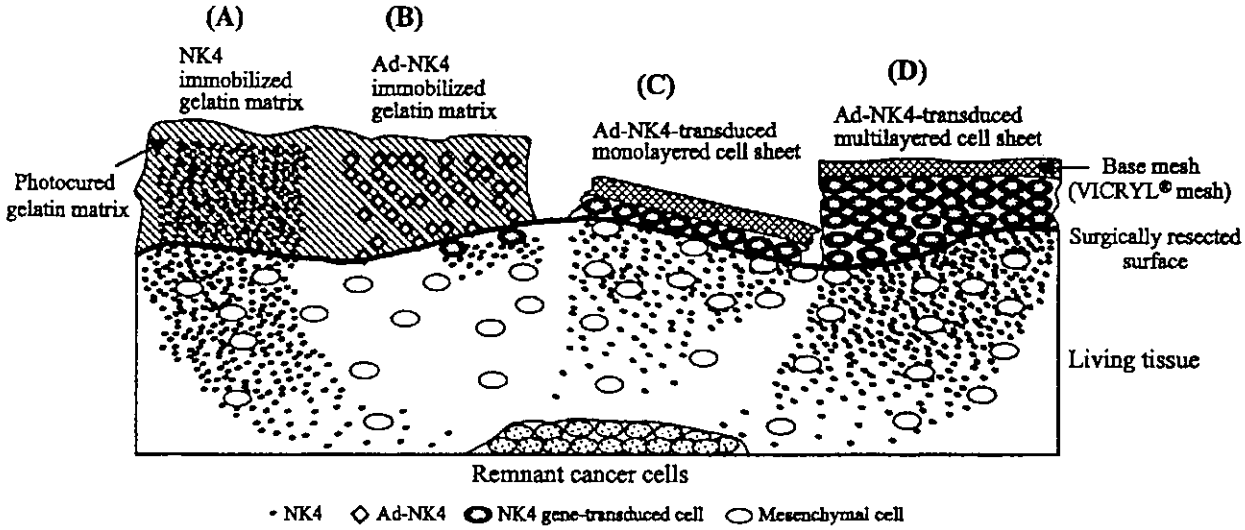

Fig. 10. Schematic of local protein delivery methods under development. (A) NK4-immobilized photocured gelatinous matrix. (B) Ad-NK4-immobilized photocured gelatinous matrix. (C) Ad-NK4-transduced monolayered cell sheet. (D) Ad-NK4-transduced multilayered cell sheet.

that the gene-transduced cell were found to be limited to on and just beneath the tissue surface. Therefore, it is highly anticipated that passive trans-tissue permeation of adenovirus, which is a giant macromolecules as compared with proteins, appears not to be effective for gene delivery [47,48]. Fig. 10 illustrates schematics of NK4- and Ad-NK4-immobilized gel layers and trans-tissue transport of NK4.

2.3. Gemcitabine (GEM) [22]

The in vitro release profile of GEM (MW; 299 g/mol) from a GEM-loaded ST-gelatin gel was characterized by an initial burst and subsequent gradual release over a prolonged period, similar to that of r-Alb from the gel. In an in vivo model using subcutaneous tumor-bearing athymic mice, rhodamine B (MW; 479 g/mol, used as a model drug of GEM) released from the ST-gelatin gel remained in the tumor at least for 10 days after photogelation on the inoculated tumor. When a GEM-loaded ST-gelatin was formed by injection, followed by subsequent photopolymerization on the inoculated tumor, the growth of the tumor was significantly suppressed without obvious adverse effects, as compared with simple GEM injection (Fig. 9B). Such suppression of tumor growth correlated with decreased cell proliferation and increased cell apoptosis in tumor cells, supported by PCNA (for proliferating cells) and TUNEL (for apoptosed cells) staining. Therefore, this strategy is considered to be highly prospective. A possible disadvantage of this system is difficulty of realization of appropriate drug-releasing profile: an adverse effect resulting from an "overdose", weak therapeutic effect due to too low dose and short releasing period due to no recharging function.

3. System II: antibody-fixed gelatinous gel (cytokine barrier) [23]

A styrene-derivatized antibody (ST-Ab), prepared with minimal affinity loss, was photocopolymerized with ST-gelatin to produce a tissue-adhesive, in situ-formed co-gel of ST-gelatin and ST-Ab, which is designed to act as a cytokine scavenger, neutralizer or barrier. A double-chamber invasion assay using an anti-HGF antibody showed that the co-gel prevented the HGF-dependent invasion of pancreatic cancer cells. On the basis of such an experimental result, when a co-gel of ST-gelatin and anti-cytokine ST-Ab is produced on a target tissue, it is anticipated that it would work well as a cytokine barrier to prevent the permeation of cytokines into the target tissue (Fig. 11A and C). Such a cytokine barrier based on an anti-cytokine fixed gel might not affect distant sites, because the antibodies were fixed in the gel, resulting in little release of the antibodies. On the other hand,

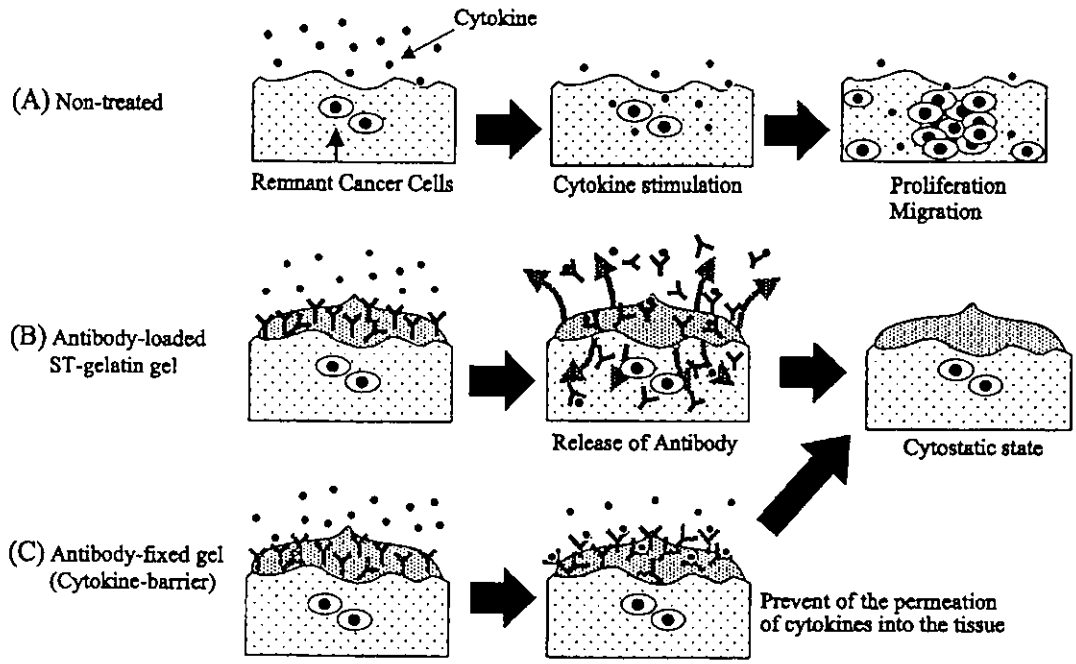

Fig. 11. Schematic of the strategy of a cytokine barrier (System II). (A) Various cytokines, produced in the intraperitoneal space during wound healing after abdominal surgery, affect remnant cancer cells in surgically resected tissues. (B) Antibody-loaded ST-gelatin gel on resected tissues. Antibodies are released from the gel, neutralize cytokines in and out of a gel, and prevent the effect of cytokines on remnant cancer cells. (C) The co-gel prepared by copolymerization of ST-gelatin and anti-cytokine ST-antibody on resected tissues. Antibodies fixed in a gel neutralize cytokines, which permeated into a gel, thereby preventing the permeation and penetration of cytokines into resected tissues [23].

when an antibody-mixed ST-gelatin solution was photogelled on a target tissue, antibodies were released from the gel and neutralized the cytokines as described above. The prevention of the permeation of cytokine into the tissue apparently results in a cytostatic state (Fig. 11). The co-gel could also be used as a drug-release matrix, from which GEM, NK4, or cytokine antibody could be released.

4. System III: cell-based delivery [24]

A hybrid tissue composed of ex vivo *NK4* gene-transduced cells was prepared for the in situ production of NK4 on a target tissue (Figs. 10C and 12). The cell source used was oral mucosal epithelial cells (OMECs), which were found to be suited to NK4 delivery because they do not secrete HGF and are easy to harvest from patients, and have reasonably high proliferation potential. OMECs were seeded on a collagen mesh-overlayered, biodegradable VICRYL® mesh, and subsequently transduced using Ad-NK4 to produce the hybrid tissue composed of NK4 gene-transduced OMECs (OMEC sheet, Fig. 12). Heterotopically implanted gene-transduced OMECs remained for at least 10 days while gradually decreasing. In an in vivo model using subcutaneous tumor-bearing nude mice, NK4 gene-transduced OMEC sheets implanted on the tumor inhibited both tumor angiogenesis (Fig. 13B) and tumor growth (Fig. 13A). Thus, it is expected that this system, developed fully using combined tissue-engineering and genetic-engineering techniques, may have great potential as a protein delivery system to target tissue at the clinical situations. The shortcomings of a prototype technology, such as the low level and short period of NK4 production, may be overcome by high density seeding of gene-transduced cells, e.g., multilayering on a microporous matrix as schematically shown in Fig. 10D. It is highly envisaged that the combination of a high cell seeding and more powerful vector enabling longer term NK4 secretion, such as retrovirus vectors, overcome the shortcomings of the prototype cell-sheet device in

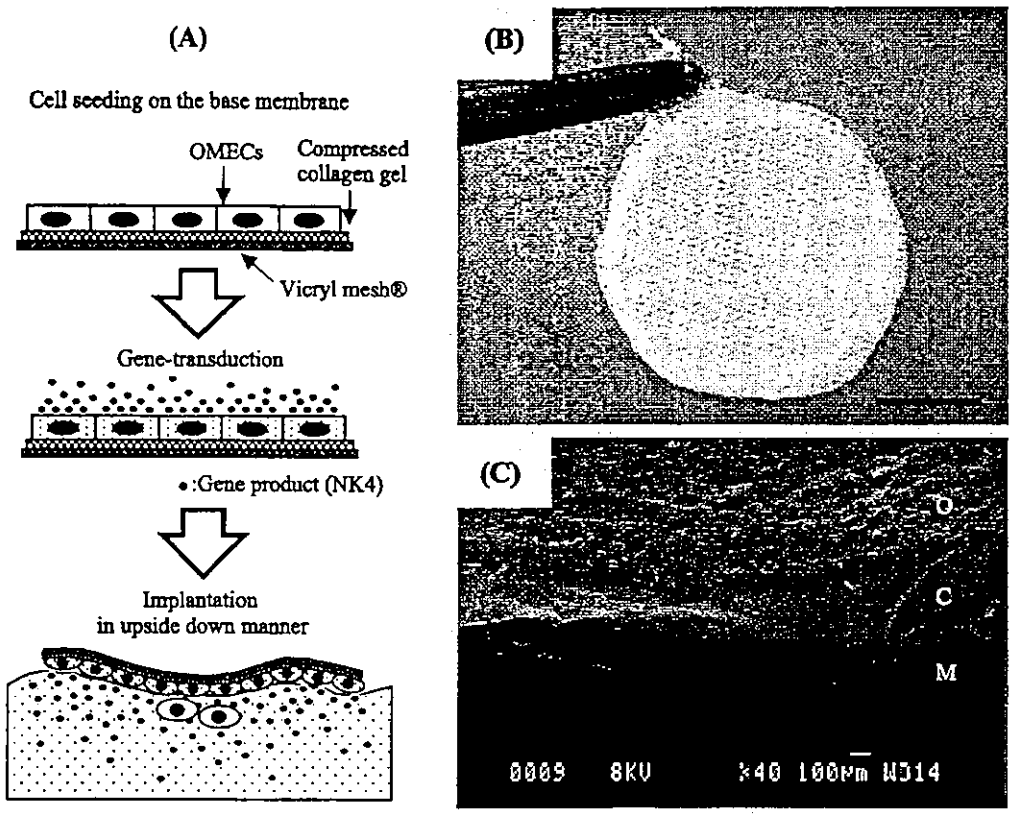

Fig. 12. System III: Cell-based delivery. (A) Schematic of gene-transduced oral mucosal epithelial cell (OMEC) sheet and the method of implantation. (B) Gross appearance of OMEC sheet. (C) Scanning electron microscopy of OMEC sheet. O, OMECs; C, collagen mesh; M, biodegradable VICRYL® mesh. Bar: 100 μm [24].

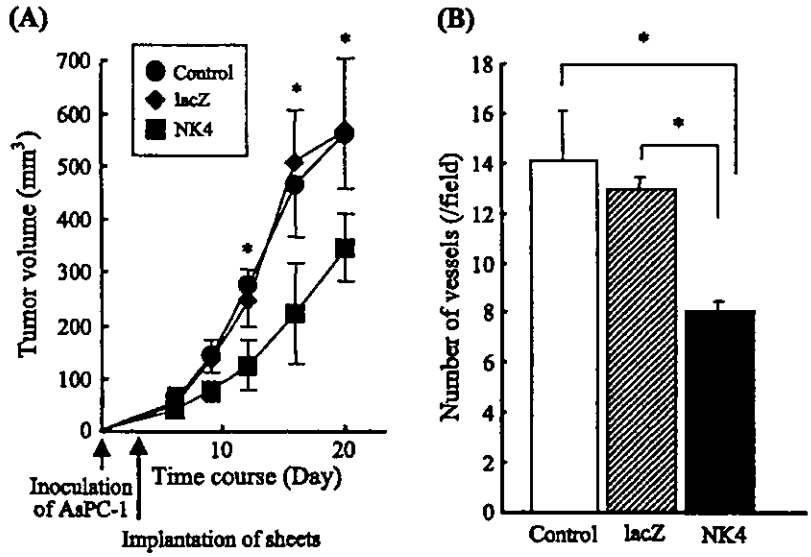

Fig. 13. Effect of NK4 gene-transduced OMEC sheet on tumor growth. Three days after cancer cell (AsPC-1) injection, tumors were covered with lacZ or NK4 gene transduced OMEC sheet. In the control group, mice were not treated. (A) Development of tumor arising from AsPC-1 cells. Values are expressed as means±S.D. (n=5, *P<0.05). (B) The number of vessels of tumors of each group. Values are expressed as means±S.D. (*P<0.05) [24].

this study. Further studies are required to increase the amount and period of in situ production of NK4.

5. System IV: device-directed delivery [25]

A rechargeable drug infusion device, which can be attached to the resected site and from which a drug is infused into the resected site, was devised (Fig. 14A). The device is composed of an elastomeric pouch (made of segmented polyurethane; SPU) having a microporous film on one side and a port connected to an elastomeric tube. The device connected to the tube guided to the extracorporeal portion permits continuous administration and recharge from the extracorporeal tube. After a few to several weeks of infusion, the device is easily removed due to the use of biodegradable sutures. The pouch is very thin (approximately 100 μm in thickness) and flexible (note that SPU, used for a diagram of artificial hearts, has proven flexibility and durability); so that the mechanically folded device is removed percutaneously through a small-sized incision upon pull-out. The prototype was fabricated with segmented polyurethane, which permits tight attachment to resected tissues using biodegradable sutures, and has multi-micropores on the side of delivery, created by a laser ablation technique coupled with computer-aided design and manufacture (Fig. 14B). In an in vivo experiment using subcutaneous tumor-bearing athymic mice, continuous infusion of GEM (150 μg/body/for 1week) from the device attached to the tumor-bearing tissue markedly suppressed tumor growth (Fig. 14C) [25]. This device, which is attached to tissue with commercially available, biodegradable sutures, can be removed easily when an adverse effect occurs or when therapy becomes unnecessary. Efforts to translate this system to the clinical situation are now underway.

6. Perspectives

The major causes of the death of patients who have undergone resection for pancreatic cancer are local recurrence and hepatic metastasis. Regarding hepatic metastasis, local chemotherapy via blood vessels has

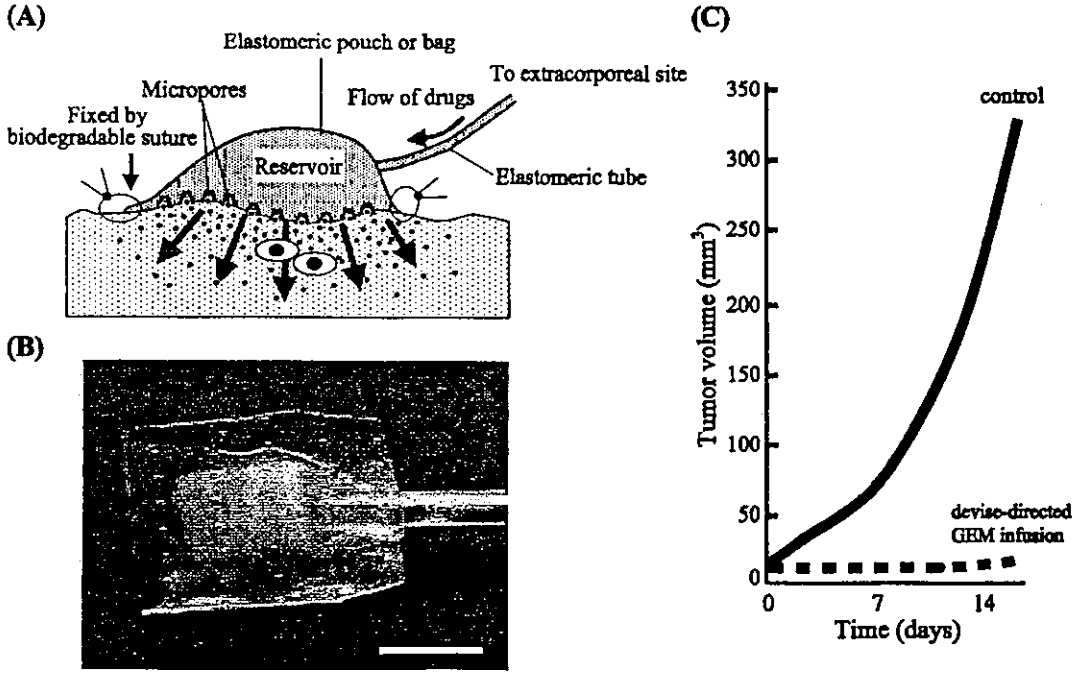

Fig. 14. System IV: Device-directed therapy. (A) Schematic of local drug delivery device. The pouch of the device is fixed on the target tissue by biodegradable sutures. Elastomeric tube connected to the pouch is guided to the extracorporeal site, which enables recharge of drugs and easy removal of the device. (B) The prototype device made by micropored segmented polyurethane. Bar: 5 mm [25]. (C) The growth of subcutaneously inoculated pancreatic cancer cell (AsPC-1). The initial tumor volume was about 20 mm^3.

been reported to reduce the occurrence of hepatic metastasis, resulting in an improvement in survival rate [40–43]. On the other hand, although several therapeutic strategies to prevent local recurrence, such as intraoperative radiotherapy, systemic chemotherapy and their combinations, have been attempted, the effect on survival rate is still under debate [9–11]. Therefore, a more effective therapeutic modality is awaited. Although a drug-delivery system used in the preclinical and clinical treatments for a variety of cancers has been reported [44–46], there have been no experimental or clinical attempts to develop a local delivery system constructed in situ on resected tissues to date. Our concept is that such a trans-tissue, local delivery system should be constructed shortly after surgical resection to minimize tumor progression caused by potent autocrine cytokines using cytostatic drugs and to enhance the cytotoxic effects of cytocidal drugs in the target tissue at very low dosage but by continuous drug exposure. For the last several years, we have been developing various new therapeutic procedures based on local drug-delivery systems as mentioned above [20–25].

Irrespective of the systems, such as a photocurable gelatinous gel (Systems I and II), a gene-transduced cell sheet (System III), and a newly devised drug-delivery device (System IV), all the therapeutic devices or materials described here can be tightly attached to the wet and uneven resected surfaces immediately after resection during surgery, and permit the local, trans-tissue delivery of various types of bioactive substances, such as anti-cancer drugs, proteins and adenoviruses, or preventing the permeation of potent tumor-progressing cytokines to the target tissue. As for the in situ gellable tissue-adhesive gel, we used photocurable gelatin which cure via visible light-induced radical polymerization of styrene group multiply derivatized on a gelatin molecule. This is originally designed to use as a hemostatic glue for surgically injured arteries during cardiovascular surgery. The rapid sol-to-gel transformation and strong tissue adhesivity withstanding against continuously loaded pulsatile stress are found to be very advantageous for trans-tissue drug delivery. Other potential candidate polymers, which meet the requirements for this particular application, may be thermoresponsible polymers which enables the sol-to-gel transformation at physiological temperature. These polymers include poly(*N*-isopropylacrylamide) or poly(ethylene glycol)–poly(propylene glycol) triblock copolymer. However, tissue adhesivity of these gels is eventually very poor due to nonionic hydrogel. In Systems I, II and IV, both cytostatic and cytocidal drugs could be delivered simultaneously, so that a more powerful synergistic effect may be expected. Caution must be paid for co-drug delivery which may cause unexpected adverse effect.

When these strategies or their combinations are applied in clinical situations as an adjuvant therapy for pancreatic cancer after thorough examination, the authors strongly envisage that the incidence of local recurrence could be reduced, hopefully resulting in a marked improvement in survival rate after surgery. To this end, research is now planned to translate these new strategic therapies in a clinical setting.

Acknowledgments

This study is financially supported by Promotion Fundamental Studies in Health Science of the Organization for Pharmaceutical Safety and Research (OPSR, contract grant number: 97-15) and Grant-in-Aid for Scientific Research from Ministry of Education, Culture, Sports, Science, and Technology of Japan (contract grant number: A2-12358017 and B2-12470277).

References

[1] T. Nakagohri, T. Kinoshita, M. Konishi, K. Inoue, S. Takahashi, Survival benefits of portal vein resection for pancreatic cancer, Am. J. Surg. 186 (2003) 149–153.
[2] T. Nagakawa, M. Nagamori, F. Futakami, Y. Tsukioka, M. Kayahara, T. Ohta, K. Ueno, I. Miyazaki, Results of extensive surgery for pancreatic carcinoma, Cancer 77 (1996) 640–645.
[3] M. Trede, G. Schwall, H.D. Saeger, Survival after pancreatoduodenectomy. 118 consecutive resections without an operative mortality, Ann. Surg. 211 (1990) 447–458.
[4] J.L. Cameron, D.W. Crist, J.V. Sitzmann, R.H. Hruban, J.K. Boitnott, A.J. Seidler, J. Coleman, Factors influencing survival after pancreaticoduodenectomy for pancreatic cancer, Am. J. Surg. 161 (1991) 120–124 (discussion 124–125).
[5] C. Sperti, C. Pasquali, A. Piccoli, S. Pedrazzoli, Recurrence after resection for ductal adenocarcinoma of the pancreas, World J. Surg. 21 (1997) 195–200.